Research article

Yanqin Miao*, Xiaozhen Wei, Long Gao, Kexiang Wang, Bo Zhao, Zhongqiang Wang, Bin Zhao, Hua Wang*, Yucheng Wu and Bingshe Xu

Tandem white organic light-emitting diodes stacked with two symmetrical emitting units simultaneously achieving superior efficiency/CRI/color stability

https://doi.org/10.1515/nanoph-2019-0175
Received June 13, 2019; revised July 19, 2019; accepted July 23, 2019

Abstract: In this work, a series of three and four-color tandem white organic light-emitting diodes (WOLEDs) are developed by using the optimized charge generating unit (CGU) to connect two electroluminescence (EL) units with symmetrical emitting layers, in which symmetrical emitting layers are constructed based on the mixed hosts; sandwiched between hole and electron-transporting hosts and the light emitted from two EL units that are absolutely complementary for forming white emission. All resulting tandem WOLEDs realize good white emission with maximum color rendering index (CRI) beyond 77 and 90 for three and four-color white devices and extremely high EL spectra stability, and also achieve high device efficiency with maximum external quantum efficiency (EQE) exceeding 33.10%. For example, for the optimized four-color tandem WOLED, the maximum CRI and EQE of 91 and 34.78% are demonstrated and only very slight CIE (Δx, Δy) variation of (0.002, −0.010) was observed at a wide luminance range from 170.9 cd/m^2 to 13,870 cd/m^2. To the best of our knowledge, this is the first tandem WOLED with only two EL units realizing such high device performances. More importantly, the proposed tandem WOLEDs here avoid introducing carrier or exciton blocking layer or using more EL units to realize high color quality white emission that provides a novel approach to develop simple, but high-performance tandem WOLEDs.

Keywords: tandem organic light-emitting diodes; white light; symmetrical emitting layer; device efficiency; color stability.

***Corresponding authors: Yanqin Miao and Hua Wang,** Key Laboratory of Interface Science and Engineering in Advanced Materials, Ministry of Education, Taiyuan University of Technology, Taiyuan 030024, China, e-mail: miaoyanqin@tyut.edu.cn (Y. Miao); wanghua001@tyut.edu.cn (H. Wang). https://orcid.org/0000-0003-2659-7696 (Y. Miao)
Xiaozhen Wei, Long Gao, Bo Zhao, Zhongqiang Wang, Yucheng Wu and Bingshe Xu: Key Laboratory of Interface Science and Engineering in Advanced Materials, Ministry of Education, Taiyuan University of Technology, Taiyuan 030024, China
Kexiang Wang: Key Laboratory of Bio-inspired Smart Interfacial Science and Technology of Ministry of Education, School of Chemistry, Beihang University, Beijing 100191, China
Bin Zhao: State Key Laboratory of Fluid Power and Mechatronic Systems, Zhejiang University, Hangzhou 310027, China

1 Introduction

White organic light-emitting diodes (WOLEDs) have attracted great attentions owing to their unique merits such as self-emitting, surface light source, flexibility, transparency, low cost, and high efficiency etc., which indicate that they have great potential applications in full-color flat-panel display and solid-state lighting fields [1–6]. In recent years, extensive efforts have been done on WOLEDs for achieving high device efficiency, color rendering index (CRI), and color stability that are required for lighting applications [6–12]. These extensive research works also contributed to great progress on WOLEDs, for example, some papers reported WOLEDs with external quantum efficiency (EQE) beyond 20% [6, 9, 11–14], which is considered as a statistical upper limit value for flat panel structure OLEDs [15]. A few research also demonstrated WOLEDs with very high CRI of >90, which is well above the threshold of 80 for WOLEDs applied in lighting field [7–8, 16–18].

Typically, the single and multiple-emissive layers (EMLs) device structures have been widely employed to develop high-performance WOLEDs. The structure for these devices is relatively simple and the total thickness of organic layers in these devices is only about 100–150 nm, inducing a time-efficient fabrication process [1–3, 5–12, 19–20]. However, these WOLEDs generally show short device lifetime (L_T), which can be ascribed to; (i) The thin thickness of organic layers makes them sensitive to the surface roughness and particles, and the materials in EMLs are more easily oxidized [20]; (ii) The L_T of OLEDs usually follows a power law dependence with respect to the applied current density (J) ($L_T \propto J^{-\beta}$, $1.5 < \beta < 3$) [21, 22], to reach a practical luminance of 3000–5000 cd/m^2, these white devices need higher current density, which also drastically causes a reduced device lifetime.

Another main issue for single and multiple-EMLs white devices is poor color stability originated from spectral variation with increasing operating voltage, especially for three or more color WOLEDs [1, 3, 23, 24]. For example, in single EML WOLEDs, different color emitters are doped into a host with very precise doping ratios, where a slight change in doping concentration will lead to an obvious change in EL spectra, and the excitons in emitter sites of low energy level are more easily saturated by energy transfer from high energy level emitters with increasing operating voltage, making EL spectra variation under different operating voltage [25, 26]. In multiple-EMLs WOLEDs, carrier recombination zone shift in different EMLs also leads to a huge EL spectra change with the increase of operating voltage [20, 27, 28]. Indeed, the introduction of carrier or exciton blocking layer can effectively improve the color stability of multiple-EMLs WOLEDs, but such device structures generally cause a decrease in device efficiency [23, 27]. Especially, for three or more color white devices, it is still hard to realize a good trade-off between device efficiency and color stability.

Tandem OLEDs, with two or more individual EL units vertically stacked and electrically connected using charge generation unit (CGU), can effectively suppress the above-defined issues in the single and multiple-EMLs WOLEDs [20, 29–33]. On the one hand, tandem OLEDs possess a thicker thickness of organic layers and exhibit a lower current density reaching the same luminance relative to the single emitting unit devices, which contribute to a substantially improved device lifetime [29, 30]. On the other hand, in traditional tandem WOLEDs, every color EML is usually located at individual EL unit, which completely eliminates the problems of energy transfer in different emitters and carrier recombination zone shift in different EMLs, inducing obviously improved color stability [31–33]. To obtain high CRI, three or more individual EL units need to be incorporated in the same tandem WOLED. Recently, Kwon et al. fabricated three-color tandem WOLEDs containing blue, green, and red three-individual EL units by using two CGUs, and as expected the device demonstrated a maximum CRI of 93 [20]. However, this white device has a number of functional layers beyond 15, indicating very complicated device structure and long-time preparation process. Thus, making tandem WOLEDs with only two EL units to simultaneously achieve extremely high efficiency/CRI/color stability is still a challenge.

In this work, we have proposed a novel tandem white device structure, where the tandem white devices contain only two EL units with complementary symmetrical EMLs (the colors emitted from EMLs are absolutely symmetrical), and a series of three and four-color tandem WOLEDs based proposed novel device structure were developed. All resulting tandem WOLEDs realize good white emission with maximum CRI beyond 77 and 90 for three and four-color white devices, respectively, and also exhibit extremely high EL spectra stability at a wide luminance range from hundreds to tens of thousands. In addition, all resulting white devices also achieve high device efficiency with maximum EQE exceeding 33.10%. For example, for the optimized four-color tandem WOLED, the maximum CRI and EQE of 91 and 34.78% are demonstrated, and only very slight CIE (Δx, Δy) variation of (0.002, −0.010) is observed at a wide luminance range from 170.9 cd/m^2 to 13,870 cd/m^2.

2 Experimental

2.1 Material information

All materials involved in device fabrication were purchased through commercial sources and directly used for device fabrication without further purification. The chemical structure of organic materials and energy levels of all materials are shown in Figure 1.

2.2 Device fabrication and characterization

All OLEDs are fabricated on the pre-patterned indium tin oxide (ITO)/glass substrates, and ITO film shows a sheet resistance of 15 Ω/□. All OLEDs have an active emissive area of 3 mm × 3 mm, defined by the overlap between the front ITO anode and the rear Al cathode. The detailed device fabrication and performance test processes are displayed in Section S1 in Supporting information, which are consistent with the work, previously reported by our group [9, 17, 18]. The films transmittance was recorded by a U-3900 spectrophotometer. The EQE was calculated using the current density–voltage–luminance (J–V–L) characteristics and spectra data. All devices and films were immediately characterized after the fabrication without encapsulation in ambient atmosphere at room temperature.

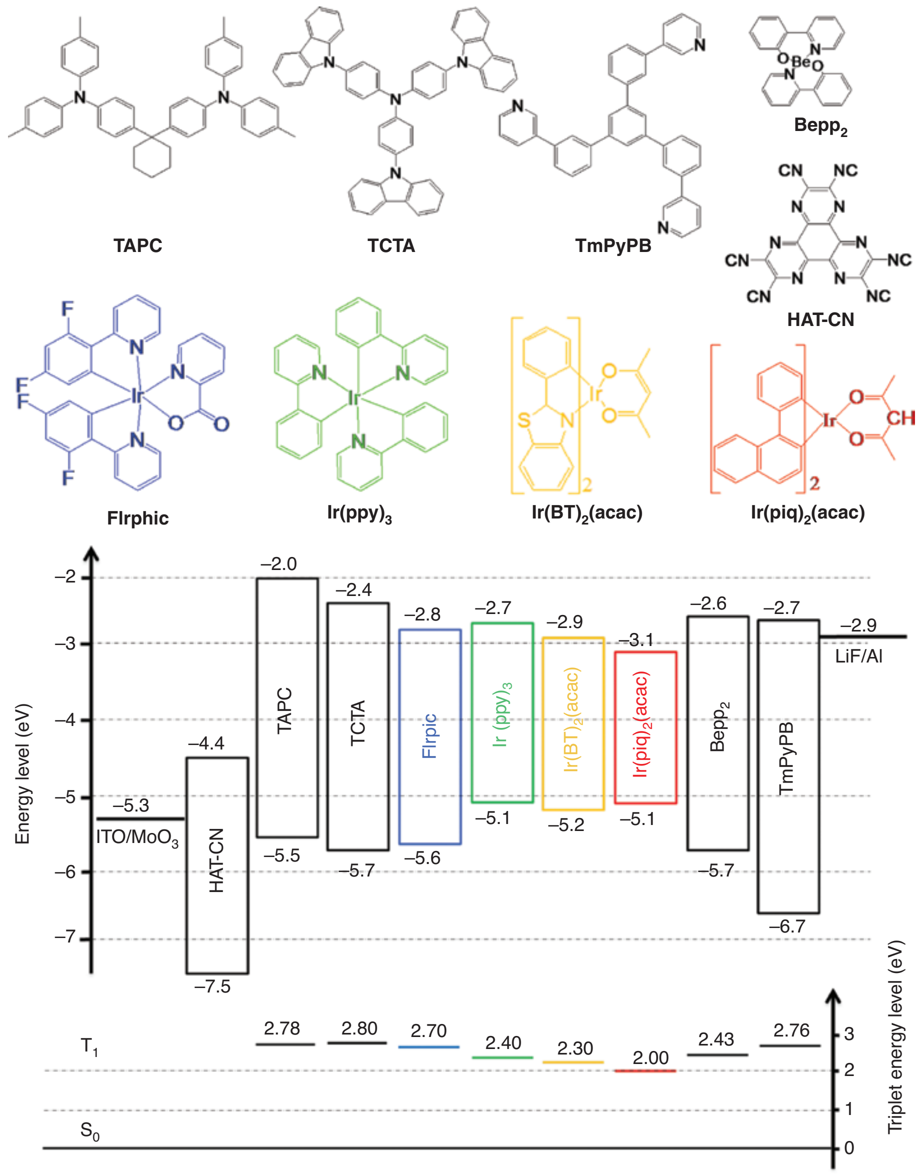

Figure 1: The chemical structure of organic materials and energy levels of all materials involved in this work.

3 Results and discussion

3.1 Optimization of charge generation unit

To realize high performance tandem OLEDs, an effective CGU is the prerequisite [29, 30, 32]. We have noted that recently, Ma et al. reported a novel CGU composition consisting of 1,4,5,8,9,11-hexaazatriphenylene hexacarbonitrile (HAT-CN) and 4,40-cyclohexylidenebis[N,N-bis(p-tolyl)aniline] (TAPC), and demonstrated a series of highly efficient tandem monochrome and white OLEDs [34, 35]. Here, we employed the similar CGU of LiF/Al/HAT-CN/HAT-CN:TAPC as in the work reported by Ma et al. [35], and demonstrated a series of tandem blue OLEDs by optimizing the thickness of Al film in the CGU. The detailed device structure is ITO(180 nm)/HAT-CN(5 nm)/TAPC(40 nm)/4,4′,4″-Tris(carbazol-9-yl)triphenylamine (TCTA):1,3,5-Tri[(3-pyridyl)-phen-3-yl]benzene (TmPyPB) (1:1): 15wt% bis(3,5-difluoro-2-(2-pyridyl) phenyl -(2-carboxypyridyl) iridium(III) (FIrpic) (20 nm)/TmPyPB(15 nm)/TmPyPB: 10wt%LiF(25 nm)/LiF(1 nm)/Al(χ nm)/HAT-CN(10 nm)/HAT-CN: TAPC(2:1, 80 nm)/TAPC(40 nm)/TCTA:TmPyPB (1:1): 15wt%FIrpic(20 nm)/TmPyPB(15 nm)/TmPyPB: 10wt%LiF(25 nm)/LiF(1 nm)/Al(100 nm), where χ = 1, 3, 5, and 7 corresponding to devices B1, B2, B3, and B4, respectively, and the device structure diagrams are shown in Figure S1 in Supporting

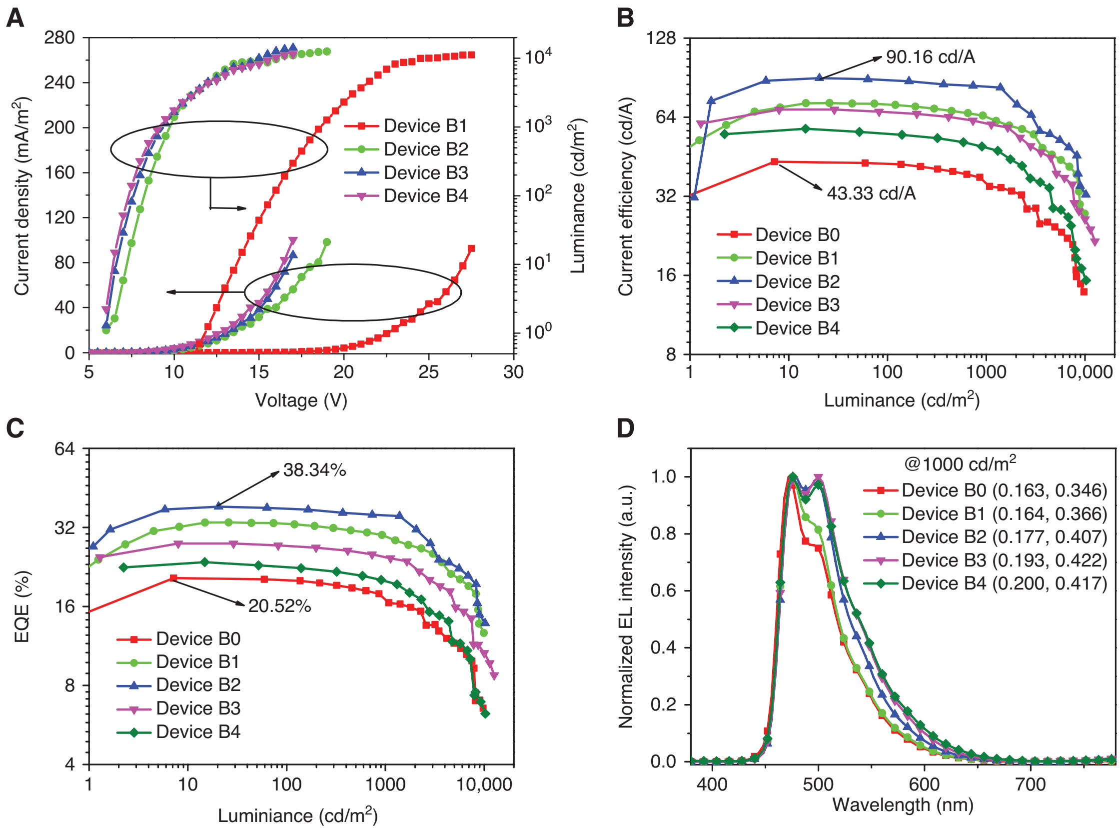

Figure 2: (A) The J-V-L curves of tandem blue devices B1–B4; (B) The CE–L (B) and EQE–L (C) curves of all single unit and tandem blue devices B0–B4; (D) The EL spectra and CIE coordinates of all single unit and tandem blue devices B0–B4 at 1000 cd/m². The single unit reference device B0 is ITO(180 nm)/HAT-CN(5 nm)/TAPC(40 nm)/TCTA:TmPyPB (1:1): 15 wt%FIrpic(20 nm)/TmPyPB(15 nm)/TmPyPB: 10 wt%LiF(25 nm)/LiF(1 nm)/Al(100 nm).

Table 1: The EL performance parameters summary of all blue OLEDs involved in this paper.

Device	V_{on}[a] (V)	Maximum			CIE[b]	Peak[b]
		CE (cd/A)	PE (lm/W)	EQE (%)		
B0	3.0	43.33	45.37	20.52	(0.163, 0.346)	472
B1	12.0	72.52	16.25	33.44	(0.165, 0.367)	476
B2	6.0	90.16	39.51	38.38	(0.177, 0.407)	476
B3	6.0	68.41	33.06	27.81	(0.193, 0.422)	476
B4	6.0	57.88	28.92	23.59	(0.200, 0.417)	476

[a]Turn-on voltage estimated at a brightness of >1 cd/m².
[b]CIE and peak values measured at a luminance of 1000 cd/m².

information. These devices are used to further optimize the charge generation and extraction ability of CGU, and the objective is to obtain an optimal CGU applied in tandem WOLEDs fabrication later. In these devices, except for the CGU of LiF(1 nm)/Al(χ nm)/HAT-CN(10 nm)/HAT-CN: TAPC(2:1, 80 nm), 5 nm-thick HAT-CN layer is used as a hole injection layer; 40 nm-thick TAPC layer is used as a hole transporting layer; 20 nm-thick TCTA:TmPyPB(1:1): 15wt%FIrpic layer is used as a blue EML; 15 nm thick TmPyPB layer and 25 nm thick TmPyPB: 10wt%LiF layer together used as an electron transporting layer; 1 nm thick LiF layer is used as electron injection layer; ITO(180 nm) and Al(100 nm) are used as anode and cathode, respectively.

Figure 2 reveals the J–V–L (except for device B0 shown in Figure S2), current efficiency – luminance (CE–L), and EQE–luminance (EQE – L) characteristic curves and EL spectra of all single unit blue device B0 and

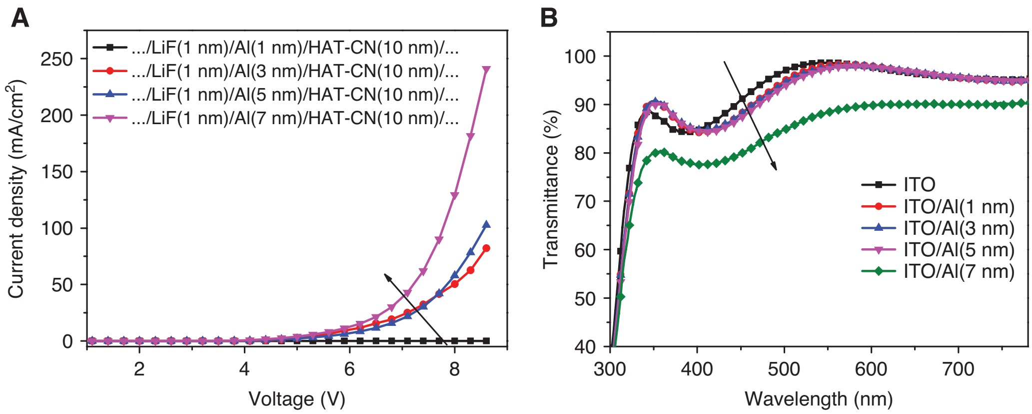

Figure 3: (A) The J–V curves of carrier-only devices based the CGU with different Al film thickness of 1, 3, 5, and 7 nm; (B) the transmittance curves of ITO(180 nm) and ITO(180 nm)/Al(1, 3, 5, and 7nm) layers.

tandem blue devices B1–B4. The detailed performance parameters for all blue devices are also summarized in Table 1. Clearly, with the increase of thickness for Al film from 1 to 7 nm, the current density for corresponding blue devices B1–B4 shows an increasing trend under the same voltage, which is attributed to an enhanced electron extraction ability from CGU to adjacent TmPyPB:LiF layer because of thicker Al film [35]. This is further verified by the carrier-only devices of ITO/TmPyPB(15 nm)/TmPyPB: 10wt% LiF(25 nm)/LiF(1 nm)/Al(1, 3, 5, and 7 nm)/HAT-CN (10 nm)/HAT-CN:TAPC (2:1, 80 nm)/TAPC(40 nm)/Al(100 nm), where the current density for these devices reveals a highly consistent increasing trend as the case in devices B1–B4 as increasing Al film thickness, shown in Figure 3A. However, from Figure 2B–C and Table 1, the maximum device efficiencies [CE, EQE, and power efficiency (PE)] for devices B1–B4 exhibit a trend of increasing first and then decreasing. This is because the increasing thickness of Al film leads to a reducing transmittance of CGU, which is also confirmed by the transmittance testing of ITO and ITO/Al(1, 3, 5, and 7 nm) layers in Figures 3B and 2D, it is observed the EL spectra from devices B0 to B4 present relatively increased shoulder peak at about 496 nm, which is attributed to the enhanced micro-cavity effect because of the reducing transmittance for CGU as the increasing thickness of Al film [36, 37]. In terms of the above comparison, the tandem blue device B2 with 3 nm thick Al film in CGU, realizes the best EL performance. For example, the device B2 shows a relatively low turn-on voltage of 6 V and the maximum CE, EQE, and PE reach 90.16 cd/A, 38.38%, and 39.51 lm/W, where the CE for device B2 is higher than the 2-fold of CE for the reference device B0. Such results indicate the optimized LiF(1 nm)/Al(3 nm)/HAT-CN(10 nm)/HAT-CN:TAPC(2:1, 80 nm) unit is a very effective CGU, which can be well employed to develop high-performance tandem WOLEDs later.

3.2 Single unit WOLEDs with symmetrical EMLs

In the previous work, we demonstrated the sandwich host structure, with mixed hosts sandwiched between hole and electron-transporting hosts, can well limit carrier recombination zone in the mixed-host layer located at the middle, and the carrier recombination zone is independent on the driving voltage, which are beneficial for structuring WOLEDs [38]. If two different emitters are doped in the middle and sides of sandwich host layer to form symmetrical EMLs WOLEDs, for example, the typical yellow/blue/yellow (Y/B/Y)-symmetrical EMLs WOLED, which can realize high efficiency and high color stability two-color white emission. Further, using CGU to connect two complementary single unit WOLEDs with symmetrical EMLs [e.g. Y/B/Y- and red/yellow/red (R/Y/R)-symmetrical EMLs single unit WOLEDs or Y/B/Y- and red/green/red (R/G/R)-symmetrical EMLs single unit WOLEDs], the resulting tandem OLEDs with only two EL units can theoretically realize three-color or four-color white emission for high color quality, and they also could combine the advantage of high efficiency and color stability for symmetrical EMLs single unit WOLEDs. Based on the above analysis, we first prepared the Y/B/Y (device S1)-, R/G/R (device S2)-, and R/Y/R (device S3)-symmetrical EMLs single unit WOLEDs and investigate their EL performance, and their device structure diagrams are shown in Figure 4.

In these devices, except for symmetrical EMLs located in the middle of the devices, other layers serve the same function as the above blue devices. In symmetrical EMLs,

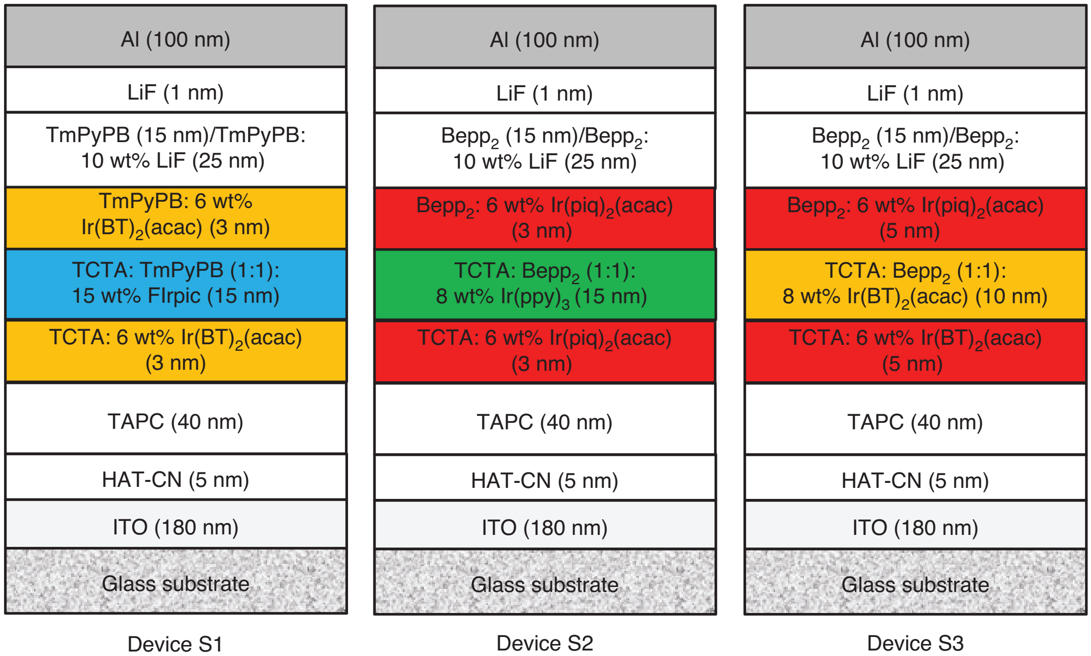

Figure 4: The device structure diagrams of symmetrical EMLs single unit WOLEDs S1–S3.

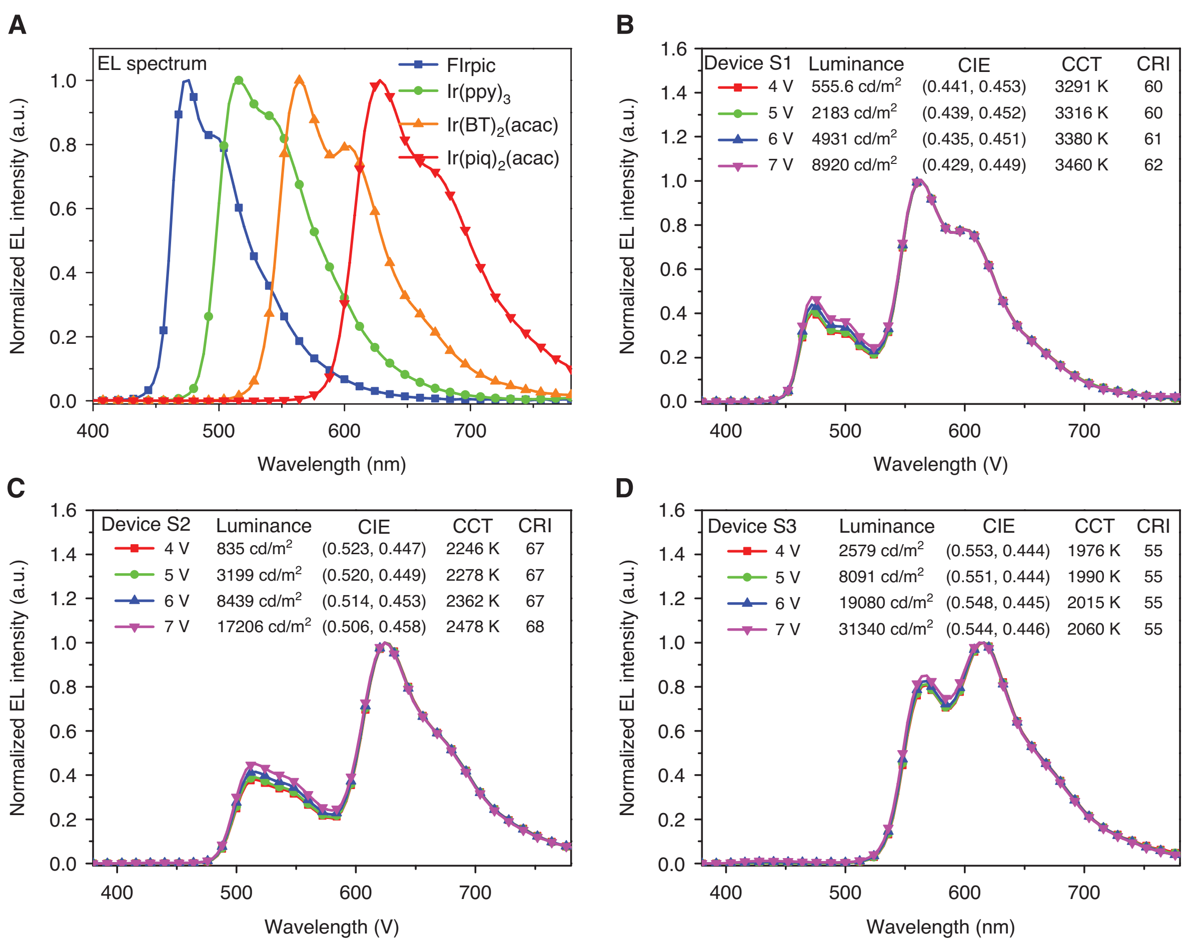

Figure 5: (A) The EL spectra of FIrpic, Ir(ppy)$_3$, Ir(BT)$_2$(acac), and Ir(piq)$_2$(acac) based monochrome OLEDs; (B–D) The EL spectra of all single unit white devices S1–S3, and luminance, CIE coordinates, CCT, and CRI of these device at different voltages are also listed.

Table 2: The EL performance parameters summary of single unit white devices S1–S3.

Device	V_{on}[a] (V)	Maximum				CIE(x, y)[c]	CCT(K)[c]	CRI[c]
		L[b] (cd/m²)	CE (cd/A)	PE (lm/W)	EQE (%)			
S1	2.8	19,620	58.06	60.80	22.11	(0.439, 0.452)	3316	60
S2	2.7	54,380	24.86	28.34	16.68	(0.520, 0.449)	2278	67
S3	2.8	56,150	40.80	47.45	19.89	(0.551, 0.444)	1990	55

[a]Turn-on voltage estimated at a brightness of >1 cd/m².
[b]L is the abbreviation of luminance.
[c]CIE, CCT, and CRI values measured at 5 V.

TACT serve as hole-transporting hosts; TmPyPB (in device S1) and Bis(2-(2-hydroxyphenyl) -pyridine)beryllium ($Bepp_2$) (in device S2 and S3) serve as electron-transporting hosts; Bis(3,5-difluoro-2-(2-pyridyl)phenyl-(2-carboxypyridyl)iridium(III) (FIrpic), tris(2-phenylpyridine)iridium(III) ($Ir(ppy)_3$), bis(2-phenylbenzothiazolato)(acetylacetonate) iridium(III) ($Ir(BT)_2(acac)$), and bis(1-phenylisoquinoline) (acetylacetonate)iridium(III) ($Ir(piq)_2(acac)$) are employed as blue, green, yellow, and red emitters, respectively. In Figure 5A, it can be seen that the EL spectra for FIrpic, $Ir(ppy)_3$, $Ir(BT)_2(acac)$, and $Ir(piq)_2(acac)$ based monochrome OLEDs cover almost all visible wavelengths from 380 to 780 nm, indicating the device, using four emitters, can obtain the broad spectrum white emission for high color quality [4, 8].

Figure 5B–D shows the EL spectra of all single unit white devices S1–S3, where the luminance, CIE coordinates, correlated color temperature (CCT), and CRI of these devices at different voltages are also listed. The EL spectra for devices S1–S3 all contain two emission peaks which are well consistent with the individual EL emission peak of two emitters employed in corresponding individual device. As the voltage increases from 4 V to 7 V, the corresponding EL spectra for all devices S1–S3 are almost completely overlapping, exhibiting extremely high color stability, which is ascribed to the strictly limited carrier recombination zone by the sandwich host structure [38]. In addition, from Figure S2 in Supporting information and Table 2, all devices S1–S3 also achieve excellent EL performance. For example, all devices S1–S3 show a relatively low turn-on voltage of 2.7–2.8 V, and the maximum luminance, CE, PE, and EQE reach 19,620 cd/m², 58.06 cd/A, 60.80 lm/W, and 22.11% for device S1, 54,380 cd/m², 24.86 cd/A, 28.34 lm/W, and 16.68% for device S2, and 56,150 cd/m², 40.80 cd/A, 47.45 lm/W, and 19.89% for device S3, respectively. The variation in EQE for three devices S1–S3 is attributed to the difference of EL performance for different emitters. Here, the achievement of high efficiency and color stability for Y/B/Y(device S1)-, R/G/R(device S2)-, and R/Y/R(device S3)-single unit WOLEDs can be ascribed to the precise management of carrier recombination zone by the sandwich host structure and they also provide the basis for developing high efficiency/CRI/color stability tandem WOLEDs later.

3.3 Tandem WOLEDs stacked with two symmetrical EL units

On the basis of obtaining optimized CGU of LiF(1 nm)/Al(3 nm)/HAT-CN(10 nm)/HAT-CN:TAPC(2:1, 80 nm) at Section 3.1 and combining the advantage of single unit WOLEDs with symmetrical EMLs, we have first developed a series of tandem three-color WOLEDs, where the devices are fabricated by using the optimized CGU to connect Y/B/Y- and R/Y/R-single unit WOLEDs, shown in Figure 6. The detailed device structure is ITO(180 nm)/HAT-CN(5 nm)/TAPC(40 nm)/TCTA: 6wt%$Ir(piq)_2(acac)$ (χ nm)/TCTA:$Bepp_2$(1:1): 8wt%$Ir(BT)_2(acac)$ (15 nm)/$Bepp_2$: 6wt%$Ir(piq)_2(acac)$(χ nm)/$Bepp_2$(15 nm)/$Bepp_2$: 10 wt% LiF(25 nm)/LiF(1 nm)/Al(3 nm)/HAT-CN(10 nm)/HAT-CN:TAPC(2:1, 80 nm)/TAPC(40 nm)/TCTA: 6wt% $Ir(BT)_2(acac)$ (χ nm)/TCTA:TmPyPB(1:1): 15wt%FIrpic(15 nm)/TmPyPB: 6wt% $Ir(BT)_2(acac)$(χ nm)/TmPyPB (15 nm)/TmPyPB: 10 wt%LiF(25 nm)/LiF(1 nm)/Al(100 nm), where χ = 2, 3, and 5 nm corresponding to tandem white devices W1, W2, and W3, respectively. In these devices, the change (χ = 2, 3, and 5) of thickness for hole and electron-transporting hosts doped with emitters layer is used to tune the EL spectra of tandem white devices for obtaining high quality white emission.

From the EL spectra of tandem WOLEDs W1–W3 in Figure 7A–C, as we expected the tandem devices W1–W3 successfully realize white emission, and the EL spectra are obviously the combination of the spectra for Y/B/Y- and R/Y/R-single unit WOLEDs, having three main emission peaks at about 476 nm, 568 nm and 616 nm, which are well originated from emissions of Firpic, $Ir(BT)_2(acac)$, and $Ir(piq)_2(acac)$, respectively [8, 38]. In addition, as χ increases from 2, 3, to 5, the corresponding white devices

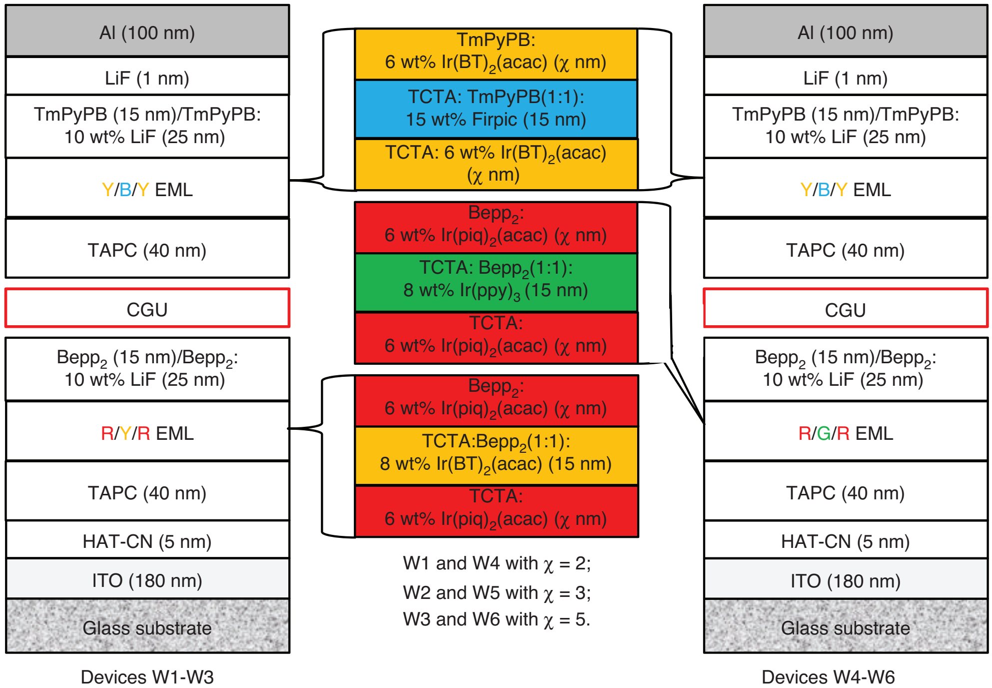

Figure 6: The device structure diagram of all tandem three-color (W1–W3) and four-color (W4–W6) WOLEDs involved in this work, where the CGU is LiF(1 nm)/Al(3 nm)/HAT-CN(10 nm)/HAT-CN:TAPC(2:1, 80 nm).

show gradually reducing blue and yellow emission intensity in EL spectra, and the reason is that the excitons generated in the middle mixed hosts EMLs can transfer more energy to the thicker yellow and red-doped EMLs on both sides. The weakened yellow intensity is because of the energy transfers from mixed hosts yellow EML to adjacent red-doped EMLs is more effective than that from the mixed hosts blue EML to adjacent yellow-doped EMLs. The reduced blue and yellow intensity contributes to an increasing CRI value, reaching 80 and 82 for device W2 and W3 in the measurable ranges [8, 17, 18]. More importantly, these tandem WOLEDs inherit well the advantages of color stability of Y/B/Y- and R/Y/R-single unit WOLEDs [20, 29, 33]. Under a wide voltage range of 7–13 V (corresponding hundreds to tens of thousands of luminance), all devices W1–W3 exhibit extremely high color stability with CIE (Δx, Δy) coordinates change of < ±0.007, ±0.011.

Figure 7D–F and Table 3, the tandem white devices W1–W3 show a slightly lower turn-on voltage of 5.5 V than the sum (5.6 V) of turn-on voltage for Y/B/Y- and R/Y/R-single unit WOLEDs owing to the effective CGU [29, 30, 34, 35]. These devices also achieve excellent EL performance with the maximum luminance, CE, PE, and EQE up to 45,010 cd/m^2, 76.37 cd/A, 39.87 lm/W, and 35.40% for device W1; 42,210 cd/m^2, 66.06 cd/A, 33.94 lm/W, and 33.42% for device W2; and 37,670 cd/m^2, 60.67 cd/A, 31.29 lm/W, and 33.10% for device W3, respectively. The slight reduced EQE from device W1 to device W3 is mainly due to a relatively lower exciton radiation efficiency for red Ir(piq)$_2$(acac) [39].

Considering relatively poor color quality for tandem three-color WOLEDs, we further prepared tandem four-color WOLEDs by using the optimized CGU to connect Y/B/Y- and R/G/R-EMLs single unit WOLEDs, shown in Figure 6. The detailed device structure is ITO(180 nm)/HAT-CN (5 nm)/TAPC (40 nm)/TCTA: 6 wt%Ir(piq)$_2$(acac) (χ nm)/TCTA:Bepp$_2$(1:1): 8 wt% Ir(ppy)$_3$(15 nm)/Bepp$_2$: 6 wt%Ir(piq)$_2$(acac)(χ nm)/Bepp$_2$(15 nm)/Bepp$_2$: 10 wt%LiF(25 nm)/LiF (1 nm)/Al (3 nm)/HAT-CN (10 nm)/HAT-CN:TAPC(2:1, 80 nm)/TAPC (40 nm)/TCTA: 6 wt% Ir(BT)$_2$(acac)(χ nm)/TCTA: TmPyPB(1:1): 15 wt%FIrpic(15 nm)/TmPyPB: 6 wt% Ir(BT)$_2$(acac)(χ nm)/TmPyPB(15 nm)/TmPyPB: 10 wt%LiF(25 nm)/LiF(1 nm)/Al (100 nm), where χ is set to 2, 3, and 5, corresponding to devices W4, W5, and W6, respectively. Here, the function for change of χ value is the same like in tandem three-color devices W1–W3.

As shown in Figure 8A–C, compared with above devices W1–W3, the tandem devices W4–W6 realize better white emission, where the EL spectra for devices W4–W6 visibly contain blue, green, yellow, and red emission peaks from FIrpic, Ir(ppy)$_3$, Ir(BT)$_2$(acac), and Ir(piq)$_2$(acac), respectively, and cover a large part (450–750 nm) of visible light band. The broad EL spectra coverage and the dominated

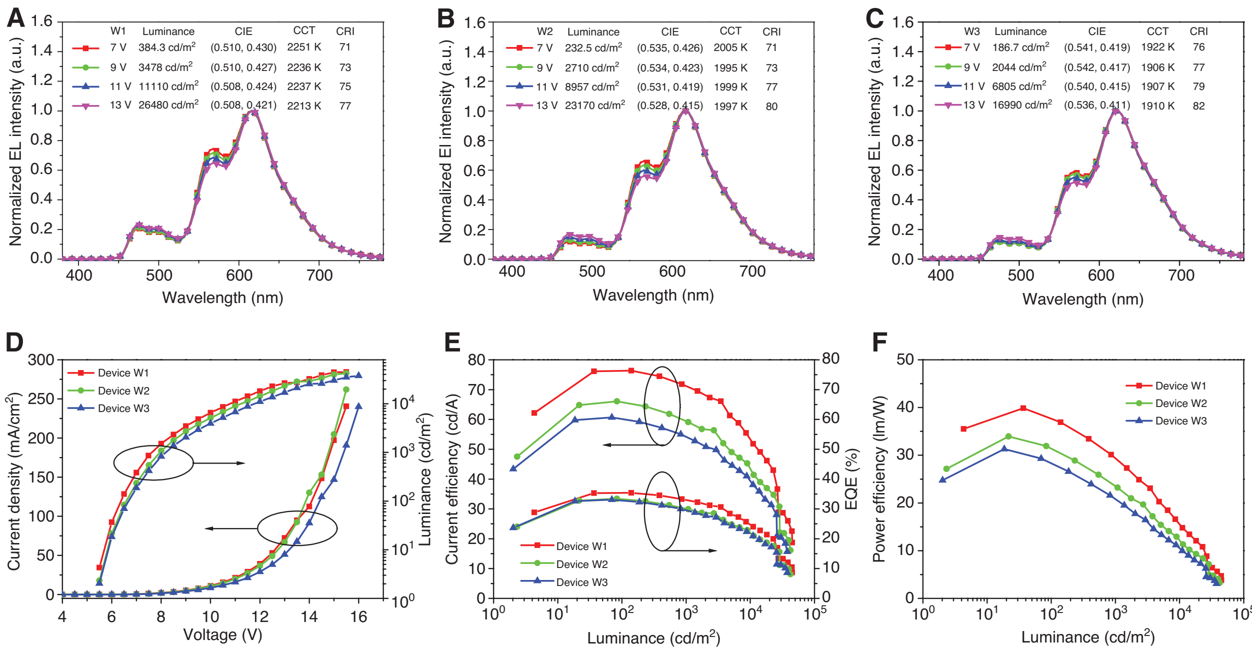

Figure 7: (A–C) The EL spectra of tandem white devices W1–W3, and luminance, CIE coordinates, CCT, and CRI of these devices at different voltages are also listed; (D–F) The J-V-L (D), CE-L-EQE (E), and PE-L curves of tandem white devices W1–W3.

Table 3: The EL performance parameters summary of three- and four-color tandem white devices W1–W6.

Device	V_{on}[a] (V)	Maximum				CIE[c]	CCT (K)[c]	CRI[c]
		L (cd/m²)[b]	CE (cd/A)	PE (lm/W)	EQE (%)			
W1	5.5	45,010	76.37	39.87	35.40	(0.508, 0.421)	2213	77
W2	5.5	42,210	66.06	33.94	33.42	(0.528, 0.415)	1997	80
W3	5.5	37,670	60.67	31.29	33.10	(0.536, 0.411)	1910	82
W4	5.5	39,070	76.16	40.16	34.78	(0.459, 0.438)	2914	91
W5	5.5	35,930	74.61	40.37	34.72	(0.480, 0.434)	2610	92
W6	5.5	27,170	66.83	34.87	33.43	(0.495, 0.425)	2382	94

[a]Turn-on voltage estimated at a brightness of >1 cd/m².
[b]L is the abbreviation of luminance.
[c]CIE, CCT, and CRI values measured at 13 V.

long band emission contribute to extremely high color quality with CCT of <3000 K and maximum CRI value of >90 for devices W4–W6 [2, 8, 24]. As χ increases from 2, 3, to 5, the corresponding devices W4–W6 present the same trend of gradually reducing emission of short-wave light (blue, green, and yellow) with an increasing CRI value, reaching 92 and 94 for device W5 and W6 at a voltage of 13 V [8, 17, 18]. The reason is consistent in the above explanation in devices W1–W3. Moreover, all devices W4–W6 also show high color stability with only very slight variation in yellow waveband in their EL spectra, especially for device W4 with CIE (Δx, Δy) coordinate change of only (0.002, −0.010) at a luminance range of 170.9–13,870 cd/m². Such repeatable striking results further demonstrate the proposed device structure and can be generally employed to develop tandem three-color or four-color WOLEDs with high color quality and color stability.

From Figure 8D–F and Table 3, it can be easily seen that tandem white devices W4–W6 also accomplish the common EL properties for universal tandem OLEDs. A low turn-on voltage of 5.5 V is obtained, which is just the sum of the turn-on voltages for above Y/B/Y- and R/G/R-single unit WOLEDs. The maximum luminance, CE, PE, and EQE reach 39,070 cd/m², 76.16 cd/A, 40.16 lm/W, and 34.78% for device W4, 35,930 cd/m², 74.61 cd/A, 40.37 lm/W, and 34.72% for device W5, and 27,170 cd/m², 66.83 cd/A, 34.87 lm/W, and 33.43% for device W6, respectively. Further, these devices also reveal relatively low efficiency roll-off.

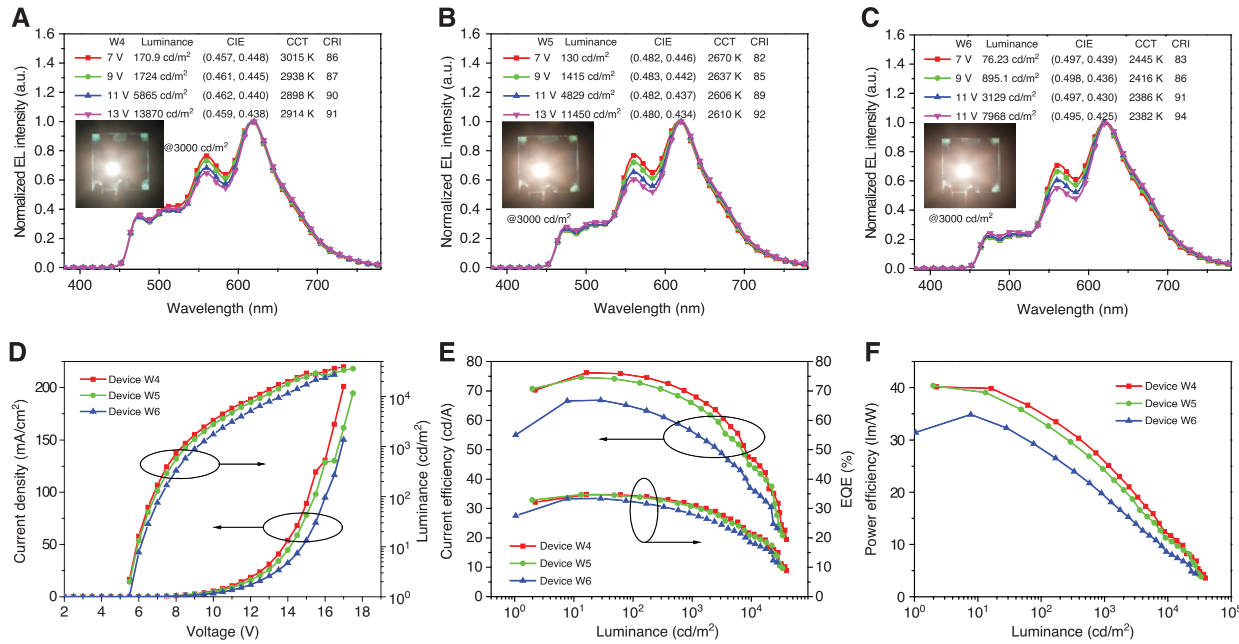

Figure 8: (A–C) The EL spectra of tandem four-color white devices W4–W6, and luminance, CIE coordinates, CCT, and CRI of these device at different voltages are also listed, and the inset in (A–C) are the photos of corresponding devices W4–W6 at a luminance of 3000 cd/m²; (D–F) The J-V-L (D), CE-L-EQE (E), and PE-L (F) curves of tandem four-color white devices W4–W6.

For example, at a practical luminance of 3000 cd/m², the CE and EQE are still up to 61.40 cd/A and 28.13% for device W4, 58.10 cd/A and 27.04% for device W5, and 49.06 cd/A and 24.73% for device W6, respectively. The optimized tandem white device W4 simultaneously achieves superior device efficiency (76.16 cd/A)/CRI (91)/color stability, which, is the first tandem white OLED with only two EL units realizing such high device performance, to the best of our knowledge [29, 34, 35, 40–48] and the detailed comparisons are shown in Table S1 in Supporting information. The achievement for such high device performance is attributed to i) an excellent charge generation ability for the optimized CGU; ii) the good management of carrier recombination zone and precise manipulation and efficient utilization of generated excitons by symmetrical EMLs [38]. It is worth mentioning that the proposed tandem white devices avoid introducing carrier or exciton blocking layer or using more EL units to realize high color quality white emission, which provides a new approach to develop simple but high-performance tandem WOLEDs.

4 Conclusions

In this work, we have proposed a novel tandem white device structure containing only two EL units with symmetrical EMLs, in which symmetrical EMLs are constructed based on the mixed hosts, sandwiched between hole and electron-transporting hosts and the light emitted from two EL units are absolutely complementary for forming white emission. Based on the above proposal novel device structure, a series of three- and four-color tandem WOLEDs are developed by using the optimized CGU to connect two EL units with symmetrical EMLs. All resulting tandem WOLEDs realize good white emission with maximum CRI beyond 77 and 90 for three and four-color white devices, respectively, and also exhibit extremely high EL spectra stability at a wide luminance range from hundreds to tens of thousands. In addition, all resulting white devices also achieve high device efficiency with maximum EQE exceeding 33.10%. For example, for the optimized four-color tandem WOLED, the maximum CRI and EQE of 91 and 34.78% are demonstrated, and an only very slight CIE (Δx, Δy) variation of (0.002, −0.010) is observed at a wide luminance range from 170.9 cd/m² to 13,870 cd/m². To the best of our knowledge, this is the first tandem WOLED with only two EL units realizing such high device performance. More importantly, the proposed tandem WOLEDs here avoid introducing carrier or exciton blocking layer or using more EL units to realize high color quality white emission, which provides a new approach to develop simple but high-performance tandem WOLEDs.

5 Supporting information

The detailed OLEDs fabrication and testing process, the structure diagram of blue device B0–B4, the J-V-L curves of device B0, the J-V-L, CE-L-EQE, and PE-L curves of singe unit white devices S1–S3.

Acknowledgments: This work was financially supported by National Natural Scientific Foundation of China (Grant No. 61705156, 61705158, 61775155, 61605137); Key Innovative Research Team in Science and Technology of Shanxi Province (Grant No. 201513002-10); Open Foundation of the State Key Laboratory of Fluid Power and Mechatronic Systems.

Conflicts of interest: There are no conflicts to declare.

References

[1] Kido J, Hongawa K, Okuyama K, et al. White light–emitting organic electroluminescent devices using the poly(N-vinylcarbazole) emitter layer doped with three fluorescent dyes. Appl Phys Lett 1994;64:815.
[2] D'Andrade BW, Forrest SR. White organic light-emitting devices for solid-state lighting. Adv Mater 2004;16:158595.
[3] Sun Y, Giebink NC, Kanno H, et al. Management of singlet and triplet excitons for efficient white organic light-emitting devices. Nature 2006;440:908–12.
[4] Sasabe H, Kido J. Development of high performance OLEDs for general lighting. J Mater Chem C 2013;1:1699.
[5] Reineke S, Lindner F, Schwartz G, et al. White organic light-emitting diodes with fluorescent tube efficiency. Nature 2009;459:234–8.
[6] Wu S, Li S, Wang Y, et al. White organic LED with a luminous efficacy exceeding 100 lm W^{-1} without light out-coupling enhancement techniques. Adv Funct Mater 2017;27:1701314.
[7] Liu B, Tao H, Wang L, et al. High-performance doping-free hybrid white organic light-emitting diodes: the exploitation of ultrathin emitting nanolayers (<1 nm). Nano Energy 2016;26:26.
[8] Miao Y, Wang K, Zhao B, et al. High-efficiency/CRI/color stability warm white organic light-emitting diodes by incorporating ultrathin phosphorescence layers in a blue fluorescence layer. Nanophotonics 2018;7:295.
[9] Miao Y, Tao P, Wang K, et al. Highly efficient red and white organic light-emitting diodes with external quantum efficiency beyond 20% by employing pyridylimidazole-based metallophosphors. ACS Appl Mater Interfaces 2017;9:37873.
[10] Wu Z, Yu L, Zhao F, et al. Precise exciton allocation for highly efficient white organic light-emitting diodes with low efficiency roll-off based on blue thermally activated delayed fluorescent exciplex emission. Adv Optical Mater 2017;5:1700415.
[11] Zhao J, Yuan S, Du X, et al. White OLEDs with an EQE of 21% at 5000 cd m^{-2} and ultra high color stability based on exciplex host. Adv Optical Mater 2018;6:1800825.
[12] Ding H, Li J, Xie G, et al. An AIEgen-based 3D covalent organic framework for white light-emitting diodes. Nat Commun 2018;9:5234.
[13] Chen B, Liu B, Zeng J, et al. Efficient bipolar blue AIEgens for high-performance nondoped blue OLEDs and hybrid white OLEDs. Adv Funct Mater 2018;28:1803369.
[14] Miao Y, Tao P, Gao L, et al. Highly efficient chlorine functionalized blue Iridium(III) phosphors for blue and white phosphorescent organic light-emitting diodes with external quantum efficiency exceeding 20%. J Mater Chem C 2018;6:6656.
[15] Lee S, Kim KH, Limbach D, et al. Low roll-off and high efficiency orange organic light emitting diodes with controlled co-doping of green and red phosphorescent dopants in an exciplex forming co-host. Adv Funct Mater 2013;23:4105.
[16] Miao Y, Wang K, Gao L, et al. Non-phosphor-doped fluorescent/phosphorescent hybrid white organic light-emitting diodes with a sandwiched blue emitting layer for simultaneously achieving superior device efficiency and color quality. J Mater Chem C 2018;6:9811.
[17] Miao Y, Wang K, Gao L, et al. Combining emissions of hole- and electron-transporting layers simultaneously for simple blue and white organic light-emitting diodes with superior device performance. J Mater Chem C 2018;6:853.
[18] Miao Y, Wang K, Zhao B, et al. Manipulation and exploitation of singlet and triplet excitons for hybrid white organic light-emitting diodes with superior efficiency/CRI/color stability. J Mater Chem C 2017;5:12474.
[19] D'Andrade BW, Holmes RJ, Forrest SR. Efficient organic electrophosphorescent white-light-emitting device with a triple doped emissive layer. Adv Mater 2004;16:624.
[20] Park MJ, Son YH, Yang HI, et al. Optical design and optimization of highly efficient sunlight-like three-stacked warm white organic light emitting diodes. ACS Photonics 2018;5:655.
[21] Murawski C, Leo K, Gather MC. Efficiency roll-off in organic light-emitting diodes. Adv Mater 2013;25:6801.
[22] Meerheim R, Scholz S, Olthof SS, et al. Influence of charge balance and exciton distribution on efficiency and lifetime of phosphorescent organic light-emitting devices. J Appl Phys 2008;104:14510.
[23] Zhang S, Yue S, Wu Q, et al. Color stable multilayer all-phosphor white organic light-emitting diodes with excellent color quality. Org Electron 2013;14:2014–22.
[24] Chang Y, Lu Z. White organic light-emitting diodes for solid-state lighting. J Disp Technol 2013;9:459.
[25] Ye J, Zheng C, Ou X, et al. Management of singlet and triplet excitons in a single emission layer: a simple approach for a high-efficiency fluorescence/phosphorescence hybrid white organic light-emitting device. Adv Mater 2012;24:3410.
[26] Tao P, Miao Y, Wang H, et al. High-performance organic electroluminescence: design from organic light-emitting materials to devices. Chem Rec 2018; DOI: 10.1002/tcr.201800139.
[27] Son YH, Park MJ, Kim YJ, et al. Color stable phosphorescent white organic light-emitting diodes with double emissive layer structure. Org Electron 2013;14:1183.
[28] Park YS, Kang JW, Kang DM, et al. Efficient, color stable white organic light-emitting diode based on high energy level yellowish-green dopants. Adv Mater 2008;20:1957.
[29] Fung MK, Li YQ, Liao LS. Tandem organic light-emitting diodes. Adv Mater 2016;28:10381.

[30] Liao LS, Klubek KP, Tang CW. High-efficiency tandem organic light-emitting diodes. Appl Phys Lett 2004;84:167.
[31] Chang CC, Chen JF, Hwang SW. Highly efficient white organic electroluminescent devices based on tandem architecture. Appl Phys Lett 2005;87:253501.
[32] Lee TW, Noh T, Choi BK, et al. High-efficiency stacked white organic light-emitting diodes. Appl Phys Lett 2008;92:043301.
[33] Coburn C, Jeong C, Forrest SR. All-phosphorescent stacked white organic light emitting devices with a high color rendering index. ACS Photonics 2018;5:630.
[34] Dai Y, Zhang H, Zhang Z, et al. Highly efficient and stable tandem organic light-emitting devices based on HAT-CN/HAT-CN: TAPC/TAPC as a charge generation layer. J Mater Chem C 2018;3:6809.
[35] Shi C, Sun N, Wu Z, et al. High performance hybrid tandem white organic light-emitting diodes by using a novel intermediate connector. J Mater Chem C 2018;6:767.
[36] Bulović V, Khalfin VB, Gu G, et al. Weak microcavity effects in organic light-emitting devices. Phys Rev B 1998;58:3730.
[37] Wang Z, Wang J, Cai W, et al, Application of an improved ensemble local mean decomposition method for gearbox composite fault diagnosis. Complexity. 2019; DOI: 10.1155/2019/1564243.
[38] Miao Y, Wang K, Gao L, et al. Precise manipulation of the carrier recombination zone: a universal novel device structure for highly efficient monochrome and white phosphorescent organic light-emitting diodes with extremely small efficiency roll-off. J Mater Chem C 2018;6:8122.
[39] Tsuboyama A, Iwawaki H, Furugori M, et al. Homoleptic cyclometalated Iridium complexes with highly efficient red phosphorescence and application to organic light-emitting diode. J Am Chem Soc 2003;125:12971.
[40] Hung WY, Fang GC, Lin SW, et al. The First Tandem, All-exciplex-based WOLED. Sci Rep 2014;4:5161.
[41] Cho H, Joo CW, Lee J, et al. Design and fabrication of two-stack tandem-type all-phosphorescent white organic light-emitting diode for achieving high color rendering index and luminous efficacy. Opt Express 2016;24:24161.
[42] Zhang X, Zhang M, Liu M, et al. Highly efficient tandem organic light-emitting devices adopting a nondoped charge-generation unit and ultrathin emitting layers. Org Electron 2018;53:353.
[43] Liu B, Wang L, Tao H, et al. Doping-free tandem white organic light-emitting diodes. Sci Bull 2017;62:1193–200.
[44] Lee S, Shin H, Kim JJ. High-efficiency orange and tandem white organic light-emitting diodes using phosphorescent dyes with horizontally oriented emitting dipoles. Adv Mater 2014;26:5864.
[45] Yu Y, Cao C, Wu Z, et al. Improving the color-rendering index of a tandem warm white organic light-emitting device by employing a simple fabrication process. Opt Lett 2019;44:931.
[46] Huang C, Xie Y, Wu S, et al. Thermally activated delayed fluorescence-based tandem OLEDs with very high external quantum efficiency. Phys Status Solidi A 2017;214:1700240.
[47] Bin JK, Lee NY, Lee SJ, et al. Two-stacked tandem white organic light emitting diodes employing WO3 as a charge generation layer. Proc SPIE 2016;9941:99411T.
[48] Xu T, Zhou JG, Fung MK, et al. Simplified efficient warm white tandem organic light-emitting devices by ultrathin emitters using energy transfer from exciplexes. Org Electron 2018;63:369.

Supplementary Material: The online version of this article offers supplementary material (https://doi.org/10.1515/nanoph-2019-0175).